Carbohydrate Polymers 89 (2012) 676–686

Contents lists available at SciVerse ScienceDirect

Carbohydrate Polymers

journal homepage: www.elsevier.com/locate/carbpol

Influence of hydroxypropylmethylcellulose addition and homogenization conditions on properties and ageing of corn starch based films

Alberto Jiménez, María José Fabra*, Pau Talens, Amparo Chiralt

Instituto de Ingeniería de Alimentos para el Desarrollo, Departamento de Tecnología de Alimentos, Universitat Politècnica de València, Camino de Vera, s/n. 46022, Valencia, Spain

ARTICLE INFO

Article history:
Received 29 December 2011
Received in revised form 20 March 2012
Accepted 25 March 2012
Available online 2 April 2012

Keywords:
Starch
HPMC
Storage
Microstructure
Tensile properties
Barrier properties

ABSTRACT

Edible films based on corn starch, hydroxypropyl methylcellulose (HPMC) and their mixtures were prepared by using two different procedures to homogenize the film forming dispersions (rotor-stator and rotor-stator plus microfluidizer). The influence of both HPMC-starch ratio and the homogenization method on the structural, optical, tensile and barrier properties of the films was analysed. The ageing of the films was also studied by characterizing them after 5 weeks' storage. Starch re-crystallization in newly prepared and stored films was analysed by means of X-ray diffraction. HPMC-corn starch films showed phase separation of polymers, which was enhanced when microfluidization was applied to the film forming dispersion. Nevertheless, HPMC addition inhibited starch re-crystallization during storage, giving rise to more flexible films at the end of the period. Water barrier properties of starch films were hardly affected by the addition of HPMC, although oxygen permeability increased due to its poorer oxygen barrier properties.

1. Introduction

Nowadays, many researchers are focusing their work on obtaining environmentally friendly materials which are able to protect food products from spoilage but also present an adequate biodegradability. In this way, traditional petroleum-based polymers, such as polyethylene or polypropylene, are being substituted by biopolymers obtained from natural and renewable sources. These polymers are mainly polysaccharides (starch, chitosan, cellulose and its derivatives) and proteins, such as gelatin, caseinates or zein, which are generally processed to obtain edible films or coatings. These structures are thin layers of edible materials applied to food products, which play an important role in their preservation, distribution and marketing (Falguera, Quintero, Jiménez, Muñoz, & Ibarz, 2011). One of the most suitable polymers with which to substitute conventional plastics is starch due to the fact that it is able to present thermoplastic behaviour if an adequate amount of plasticizers is used. Starch is a well-known polysaccharide that presents different properties depending on its amylose/amylopectin ratio. Properties, such as glass transition temperature (Liu et al., 2010) or digestibility (resistant starch; Zhu, Liu, Wilson, Gu, & Shi, 2011), vary according to the amylose content. Their properties, as packaging material alone or in combination with other materials, have been widely studied (Bertuzzi, Armada, & Gottifredi, 2007; Chillo et al., 2008; Flores, Conte, Campos, Gerschenson, & Del Nobile, 2007; Kuorwel, Cran, Sonneveld, Miltz, & Bigger, 2011; Phan The, Debeaufort, Luu, & Voilley, 2005; Tang, Alavi, & Herald, 2008). Although starch based films and coatings generally present adequate properties, it has been found that storage greatly increases the crystalline fraction in the starch matrix (Jiménez, Fabra, Talens, & Chiralt, 2012; Mali, Grossmann, García, Martino, & Zaritzky, 2006); a fact that may lead to a deterioration of the protective ability of starch-based packaging. Jiménez et al. (2012) related the increase in crystallinity with the changes in different properties (gloss, transparency, brittleness) of the films, which can affect the film functionality and consumer acceptance of coated products. One way to avoid the recrystallization of starch is by combining this polymer with others, preferably amorphous. One of the biopolymers with this characteristic is hydroxypropyl-methylcellulose (HPMC). Its ease of use, availability, water solubility, and non-toxicity makes HPMC the most extensively used cellulose derivative (Fahs, Brogly, Bistac, & Schmitt, 2010). The amorphous state of HPMC has been reported by Kou et al. (2011) through X-ray diffraction analysis. Huang, Chen, Lin, & Chen (2011) succeeded in reducing the crystallinity index of bacterial culture cellulose by adding HPMC to the bacterial culture medium, pointing to this polymer's capacity to inhibit crystallization.

HPMC has also been studied as a matrix of edible films in combination with different components, such as fatty acids (Jiménez, Fabra, Talens, & Chiralt, 2010) or cellulose nano-particles (Bilbao-Sainz, Bras, Williams, Sénechal, & Orts, 2011). Nevertheless, there is

* Corresponding author. Tel.: +34 963877000x83613.
E-mail address: mafabro@doctor.upv.es (M.J. Fabra).

0144-8617/$ – see front matter © 2012 Elsevier Ltd. All rights reserved.
http://dx.doi.org/10.1016/j.carbpol.2012.03.075

no available literature on the mixing of HPMC with starch in order to form edible or biodegradable films or packages.

Starch is able to form films in combination with various polymers, such as agar, arabinoxylan (Phan The, Debeaufort, Voilley, & Luu, 2009) or chitosan (Bourtoom & Chinnan, 2008; Vásconez, Flores, Campos, Alvarado, & Gerschenson, 2009). Phan The et al. (2009), working on films containing mixtures of starch with agar or arabinoxylan, observed that the component integration in the matrix was greatly dependent on the type of polymer. Cassava starch-arabinoxylan film was homogeneous, whereas cassava starch-agar film showed a phase separation and dispersion.

The aim of this work was to evaluate the influence of HPMC addition, the homogenization conditions of the film forming dispersion as well as the effect of ageing on the structural, mechanical, and optical and barrier properties (water vapour and oxygen) of corn starch-glycerol based films.

2. Materials and methods

2.1. Materials

Corn starch was obtained from Roquette (Roquette Laisa España, Benifaió, Spain). Hydroxypropyl-methylcellulose (HPMC) was purchased from Fluka (Sigma–Aldrich Chemie, Steinheim, Germany). Glycerol, used as plasticizer, was provided by Panreac Quimica, S.A. (Castellar Del Vallés, Barcelona, Spain), as well as magnesium nitrate-6-hydrate which was used to equilibrate film samples at 53% RH.

2.2. Preparation and characterization of films

Eight different formulations based on corn starch and/or HPMC were prepared. Firstly, both polysaccharides were dispersed separately: HPMC was dissolved (2%, w/w) in cold water by continuous stirring and maintained under these conditions overnight, whereas dispersions containing 2% (w/w) starch were mildly stirred with a stirring rod while maintained at 95 °C for 30 min to promote polysaccharide gelatinization. Afterwards, both hydrocolloid solutions were mixed at room temperature in different ratios to obtain four dispersions with 100:0, 75:25, 50:50 and 0:100 starch:HPMC ratios. Then, the plasticizer was added using a hydrocolloid:plasticizer ratio of 1:0.25. Glycerol was chosen as plasticizer for all formulations due to it being a better plasticizer than other polyols (sorbitol and xylytol) with the same plasticizer content (Talja, Helén, Roos, & Jouppila, 2007). The homogenization of film-forming dispersions was carried out under vacuum, to avoid bubble formation, and at 95 °C using a rotor-stator homogenizer (Ultraturrax T25, Janke and Kunkel, Germany) for 1 min at 13,500 rpm and for 5 min at 20,500 rpm. A part of each formulation was also homogenized in a second step using a Microfluidizer M-110P (Microfluidics International Corp., Newton, MA, USA) at 103,390 kPa (microfluidized samples), thus obtaining eight different film forming solutions (samples A to H).

Controlled amounts of film-forming dispersions (containing 1.5 g of total solids) were spread evenly over a Teflon® casting plate (15 cm diameter) resting on a leveled surface, and films were formed by drying them for approximately 48 h at 45% RH and 20 °C. Afterwards, the dried films were peeled intact from the casting surface. Film thickness was measured with a Palmer digital micrometer to the nearest 0.0025 mm at six random positions before tests.

2.2.1. Film equilibration and storage

Prior to testing, samples were equilibrated in dessicators at 25 °C and 53% RH, by using magnesium nitrate-6-hydrate saturated solutions for one week when the first series of analyses was carried out. One part of the different samples was stored under the same conditions for five weeks, when the second series of analyses was performed.

2.2.2. Tensile properties

A universal test Machine (TA.XTplus model, Stable Micro Systems, Haslemere, England) was used to determine the tensile strength (TS), elastic modulus (EM), and elongation (E) of the films, following ASTM Standard Method D882 (ASTM, 2001) EM, TS, and E were determined from the stress–strain curves, estimated from force–distance data obtained for the different films (2.5 cm wide and 10 cm long). Six replicates were analysed per formulation. Equilibrated specimens were mounted in the film-extension grips of the testing machine and stretched at 50 mm min^{-1} until breaking. The relative humidity of the environment was maintained constant at 53 (±2)% during the tests, which were carried out at 25 (±1) °C.

2.2.3. X-ray diffraction

X-ray diffraction patterns were recorded using a Rigaku Ultima IV multipurpose X-ray diffraction system (Rigaku Corporation, Tokyo, Japan). All samples were analysed between 5° and 50° (2θ) using Kα Cu radiation (λ = 1.542 Å), 40 kV and 40 mA with a step size of 0.02°. For this analysis, samples were cut into 2 cm squares, prior to storage, in order to avoid breakage during handling. Analyses were performed at 25 °C and 53% RH. To this end, samples were equilibrated at these conditions which were also maintained in the laboratory where the X-ray difractometer was located.

2.2.4. Water vapour permeability (WVP)

A modification of the ASTM E96-95 (1995) gravimetric method (McHugh, Avena-Bustillos, & Krochta, 1993) for measuring WVP of flexible films was employed for all samples using Payne permeability cups (3.5 cm diameter, Elcometer SPRL, Hermelle/s Argenteau, Belgium). Films were selected for WVP tests based on lack of physical defects, such as cracks, bubbles, or pinholes. Each cup was filled with distilled water to expose the film to 100% RH on one side. Once the films were secured, the cups were placed in a relative humidity equilibrated cabinet fitted with a fan to provide a strong driving force across the film for water vapour diffusion. The RH of the cabinets (53% at 25 °C) was held constant using oversaturated solutions of magnesium nitrate-6-hydrate. The free film surface during film formation was always exposed to the lowest relative humidity, whereas the cabinets were maintained at 25 °C during the tests. The cups were weighed each 2 h (0.0001 g) throughout 24 h. Water vapour transmission (WVTR) was determined from the slope obtained from the regression analysis of weight loss data versus time, once the steady state had been reached, divided by the film area.

From WVTR data, the vapour pressure on the film's inner surface (p_2) was obtained using Eq. (1), proposed by McHugh et al. (1993), to correct the effect of concentration gradients established in the stagnant air gap inside the cup:

$$\mathrm{WVTR} = \frac{P \cdot D \cdot \mathrm{Ln}\ [(P - p_2)/(P - p_1)]}{R \cdot T \cdot \Delta z} \quad (1)$$

where P, total pressure (atm); D, diffusivity of water through air at 25 °C ($m^2\ s^{-1}$); R, gas law constant ($82.057 \times 10^{-3}\ m^3\ atm\ kmol^{-1}\ K^{-1}$); T, absolute temperature (K); Δz, mean height of stagnant air gap (m), considering the initial and final z values; p_1, water vapour pressure on the solution surface (atm); and p_2, corrected water vapour pressure on the film's inner surface (atm). Water vapour permeance was calculated

using Eq. (2) as a function of p_2 and p_3 (pressure on the film's outer surface in the cabinet).

$$\text{Permeance} = \frac{\text{WVTR}}{p_2 - p_3} \quad (2)$$

Permeability was obtained by multiplying the permeance by the average film thickness.

2.2.5. Oxygen permeability

The oxygen barrier properties of the films were evaluated by measuring oxygen permeability (OP) by means of an Ox-Tran 1/50 system (Mocon, Minneapolis, USA) at 25 °C (ASTM Standard Method D3985-95, 2002). Measurements were taken at 53% in films previously equilibrated at the same RH. Films were exposed to pure nitrogen flow on one side and pure oxygen flow on the other side. The OP was calculated by dividing the oxygen transmission rate by the difference in the oxygen partial pressure on the two sides of the film, and multiplying by the average film thickness. At least three replicates per formulation were considered.

2.2.6. Scanning electron microscopy (SEM)

A microstructural analysis of the films was carried out using a scanning electron microscope (JEOL JSM-5410, Japan). Film samples were maintained in a desiccator with P_2O_5 for 15 days. Then the films were frozen in liquid N_2 and gently and randomly broken to observe the cross-section and the surface of the film samples. Films were fixed on copper stubs, gold coated, and observed using an accelerating voltage of 10 kV.

2.2.7. Optical properties

The transparency of the films was determined by applying the Kubelka–Munk theory (Hutchings, 1999) for multiple scattering to the reflection spectra. The surface reflectance spectra of the films were determined from 400 to 700 nm using a spectrocolorimeter CM-3600d (Minolta Co., Tokyo, Japan) on both a white and a black background. As the light passes through the film, it is partially absorbed and scattered, which is quantified by the absorption (K) and the scattering (S) coefficients. The internal transmittance (T_i) of the films was quantified using Eq. (3). In this equation, R_0 is the reflectance of the film on an ideal black background. Parameters a and b were calculated by Eqs. (4) and (5), where R is the reflectance of the sample layer backed by a known reflectance R_g. Measurements of each sample were taken in triplicate on the free film surface during drying.

$$T_i = \sqrt{(a - R_0)^2 - b^2} \quad (3)$$

$$a = \frac{1}{2} \cdot \left(R + \frac{R_0 - R + R_g}{R_0 R_g} \right) \quad (4)$$

$$b = (a^2 - 1)^{1/2} \quad (5)$$

The gloss was measured on the free film surface during film formation, at 60° angles from the normal to the surface, following the ASTM Standard D-523 Method (1999), using a flat surface gloss meter (Multi.Gloss 268, Minolta, Germany). Measurements of each sample were taken in triplicate and three films of each formulation were considered. All results are expressed as gloss units, relative to a highly polished surface of standard black glass with a value close to 100.

2.3. Statistical analysis

Statistical analyses of data were performed through an analysis of variance (ANOVA) using Statgraphics Plus for Windows 5.1 (Manugistics Corp., Rockville, MD). Fisher's least significant difference (LSD) procedure was used at the 95% confidence level.

3. Results

3.1. Microstructural properties

The final structure of the film depends on both the interactions of film components and the drying conditions of the film-forming dispersion and has a great impact on the different film properties (Fabra, Talens, & Chiralt, 2009; Souza et al., 2009; Villalobos, Chanona, Hernández, Gutiérrez, & Chiralt, 2005). In this sense, Fabra, Jiménez, Atarés, Talens, & Chiralt (2009) showed that the microstructural analysis of the films gives relevant information about the arrangement of the components, which, in turn, allows the values obtained for the water barrier, mechanical or optical properties to be understood.

Fig. 1 shows the SEM micrographs obtained from the cross-sections of the obtained films. Generally, pure starch films (Fig. 1A and E) or pure HPMC films (Fig. 1D and H) showed a homogeneous structure, whereas a more heterogeneous structure was observed for films prepared with mixtures of both polysaccharides (75:25 or 50:50 starch:HPMC ratio). Slight differences were observed when comparing pure HPMC micrographs (Fig. 1D and H) with those reported by Jiménez et al. (2010), which can be attributed to the presence of glycerol in the present films. Cross-section images reported by Jiménez et al. (2010) for pure HPMC films (glycerol-free) were homogeneous and completely smooth, whereas irregularities in the micrographs can be observed when glycerol was added. Even in non-microfluidized samples (Fig. 1D), a different phase can be observed on the bottom of the films, indicating that glycerol is not homogenously distributed across the film. When high-pressure was applied, although the components were distributed more homogeneously in the polymer matrix, the matrix obtained was still not completely smooth. This suggests the lack of a complete miscibility of HPMC and glycerol. This is also observed in surface images shown in Fig. 2D in which different separate zones in the film surface can be appreciated in agreement with phase separation in HPMC-Gly films. Nevertheless glycerol dispersion was enhanced when the homogenization intensity increased and film surface appeared much more homogeneous (Fig. 2H).

Pure starch films showed a smooth surface and a homogeneous microstructure in the cross section images in both microfluidized and non-microfluidized films (Figs. 1A, E and 2A, E), although microfluidification yields a more brittle network as revealed by the micro-cracks provoked by the electron impact. This could be explained by a different arrangement of the amylopectin and amylose fractions in each case due to the high shear applied during microfluidification. Different authors (Paes, Yakimets, & Mitchell, 2008; Rindlav-Westling, Stading, & Gatenholm, 2002) report that amylose–amylopectin separation can occur during film formation depending on shear and temperature applied and the amylose–amylopectin ratio. A competition between gel formation and phase separation may occur in the amylose–amylopectin–water systems and, if the relative rate of phase separation is lower than the relative rate of gelation, no-phase separation occurs in the system during cooling. Rindlav-Westling et al. (2002) reported that when the amylose proportion in the amylose–amylopectin blends was lower than 25%, a phase separation occur, but at higher amylose proportions, the phase separation was apparently prevented by amylose gelation and the formation of a continuous amylose network. The amylose content in native corn starch is around 25% (García, Pinotti, Martino, & Zaritzky, 2009). Moreover, Paes et al. (2008) reported that amylose–amylopectin phase separation occurred when severe temperature and shear conditions were applied during film formation, while remnants of the granules or ghosts are present for mild temperature or shear conditions. This affects the final film microstructure and its mechanical properties.

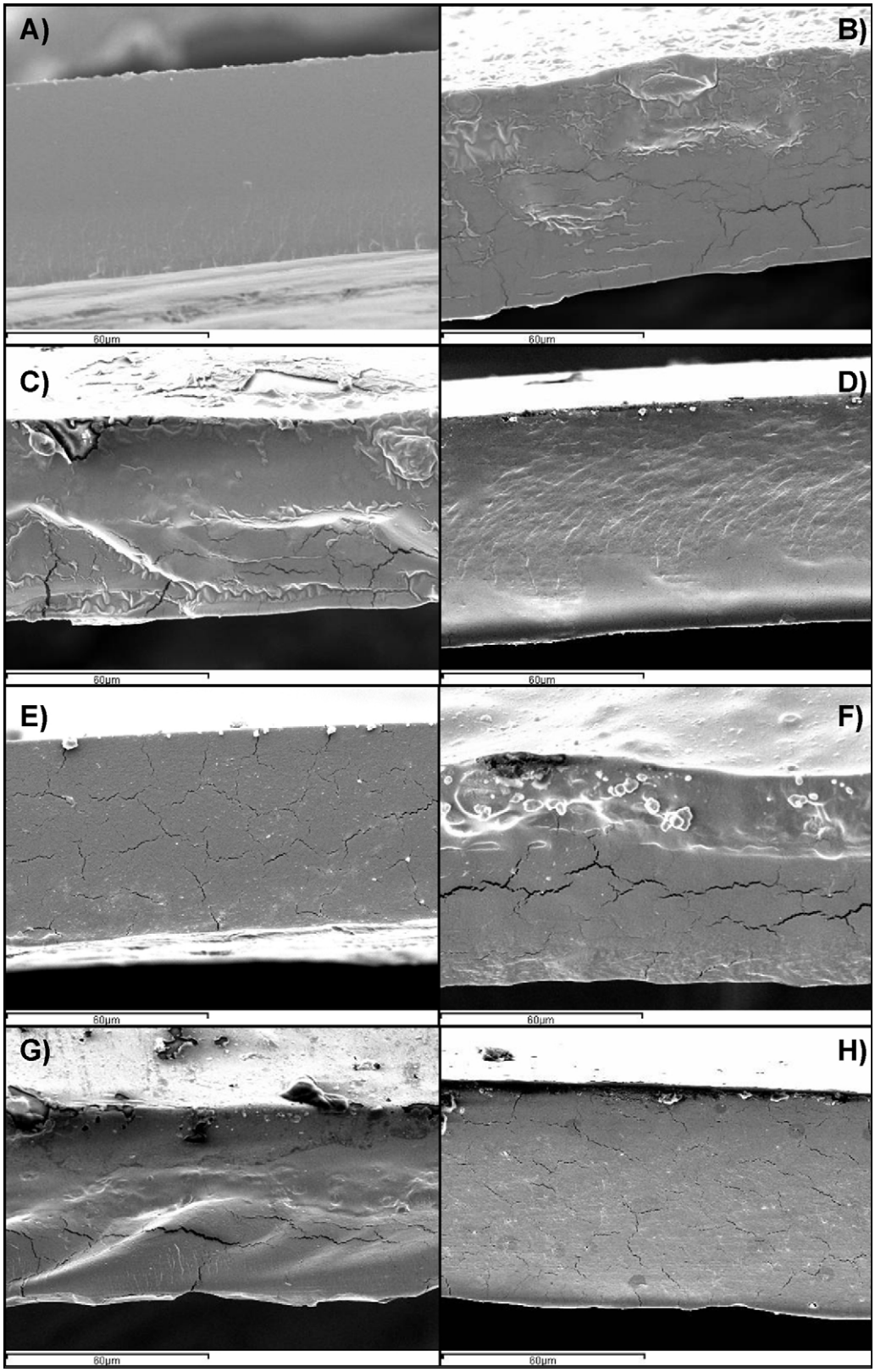

Fig. 1. SEM images of the cross-sections of the studied films. A to D correspond to non-microfluidized films, E to H correspond to microfluidized films. A and E: 100:0 starch:HPMC ratio, B and F: 75:25 starch:HPMC ratio, C and G: 50:50 starch:HPMC ratio and D and H: 0:100 starch:HPMC ratio.

Micrographs of films prepared with mixtures of both polysaccharides (starch:HPMC blends) showed a heterogeneous structure, showing phase separation between starch and HPMC due to the lack of polymer compatibility. In any case microfluidization leads to a clearer separation of two phases in the films (top and bottom), despite the high pressure applied to the film forming dispersion. These two phases will be an HPMC-enriched phase and a starch-enriched phase. The polymer incompatibility leads to films whose

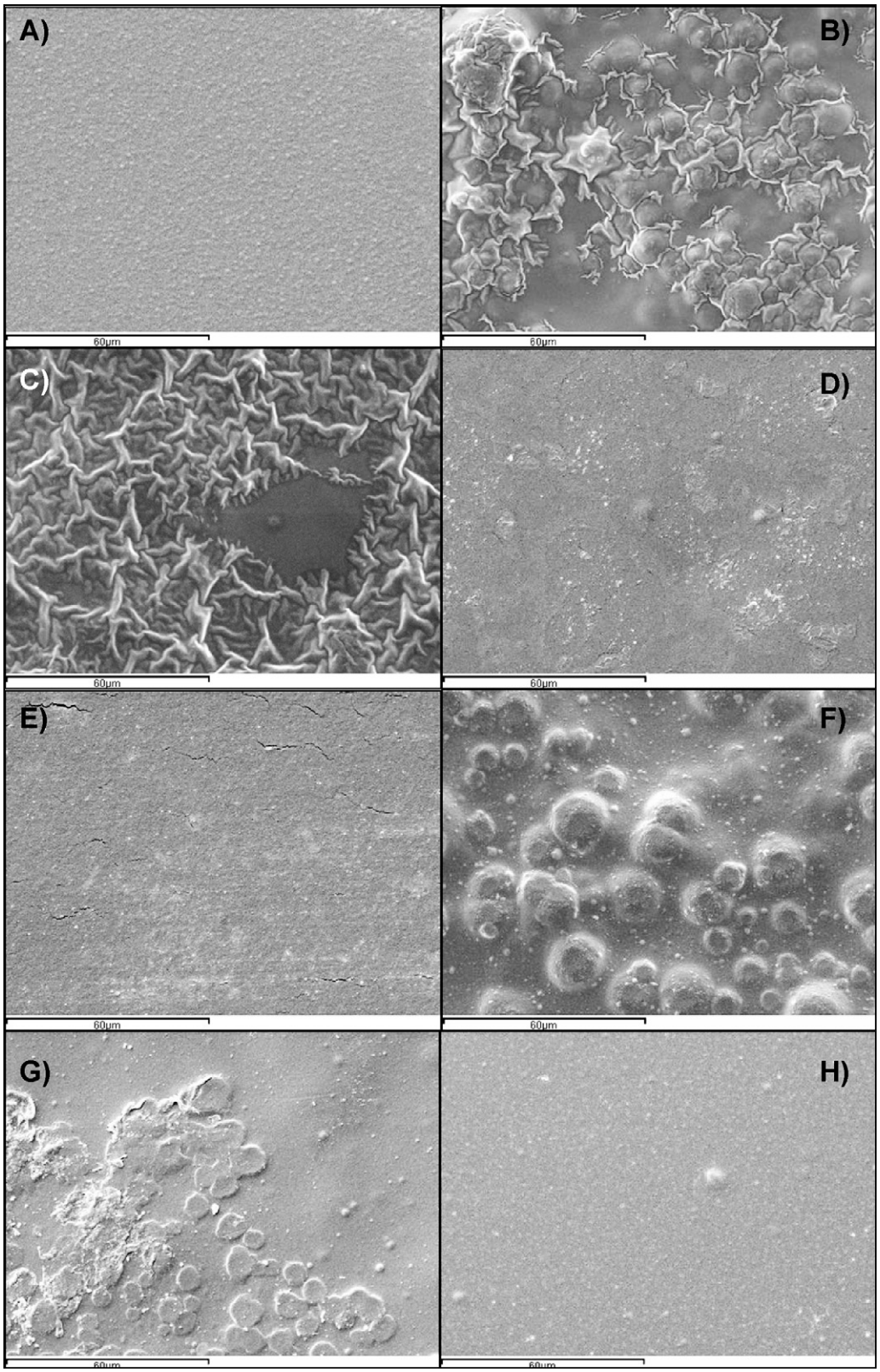

Fig. 2. SEM images of the film surface of composite films. A to D correspond to non-microfluidized films, E to H correspond to microfluidized films. A and E: 100:0 starch:HPMC ratio, B and F: 75:25 starch:HPMC ratio, C and G: 50:50 starch:HPMC ratio and D and H: 0:100 starch:HPMC ratio.

heterogeneity cannot be avoided by high pressure homogenization conditions. In fact, composite films homogenized by means of a rotor-stator showed a dispersed phase embedded in a continuous phase; however, when microfluidization was applied, phase separation was more evident probably due to the fact that the promotion of polymer chain interactions at high pressure enhances their incompatibility. From the obtained images, it could be deduced that the starch-enriched phase was located at the

bottom of the film, whereas the HPMC-enriched phase was at the top, depending on the relative density of both polymers. In this sense, it is remarkable that liquid phase separation was also visually observed in the film forming dispersions, where the starch phase (less transparent) was also appreciated at the bottom of the system.

The non-homogeneous structure of films obtained by mixing polysaccharides has been previously reported. Mathew and Abraham (2008) found that adding ferulic acid led to starch-chitosan films that were more homogeneous than others which did not have this component, which was explained by the cross-linking activity of ferulic acid. Annable, Fitton, Harris, Philips, & Williams (1994) reported that the incorporation of a hydrocolloid, such as galactomannans, into starch dispersion at a sufficiently high concentration leads to the phase separation of mixed gels into two different phases.

The internal network of these kinds of films, formed during drying, usually affects different properties. In this sense, the tortuosity of the internal structure affects the light transmission/dispersion behaviour of the film, and so its transparency–opacity ratio. In previous works, Fabra, Jiménez, et al. (2009) and Jiménez et al. (2010) found that films became less transparent when fatty acids were added to sodium caseinate and HPMC based films, due to the layered structure of these films; the more layers there are, the less transparent the film.

The film's microstructural irregularities have an impact on the surface level that greatly affects surface roughness, and so film gloss. To evaluate this impact on the composite films, SEM micrographs of the film surface were obtained. Fig. 2 shows the surface SEM micrographs of the microfluidized and non-microfluidized films. Different particles can be observed in all composite films (Fig. 2B, C, F and H). These particles are irregular in shape in films obtained with a single rotor-stator homogenization step (Fig. 2B and C) and more spherical in those obtained following a 2-step homogenization process (Fig. 2F and G). Microfluidized films show a clear reduction in surface irregularities and roughness as compared with non-microfluidized films, which coincides with the clearer phase separation observed in the film's cross-section images. Whereas punctual chain aggregates, filamentous in shape, can be observed in non-microfluidized films, in microfluidized films, spherical particles, resulting from the separation of polymer aqueous phases remain on the film surface.

3.2. Optical properties

The different structural arrangement of polysaccharides in the studied films could have an effect on their optical properties, since changes in the refractive index occur through the polymer matrix. Film transparency was evaluated by means of internal transmittance (T_i). Fig. 3 plots the spectral distribution curves of T_i for both newly prepared (a) and stored films (b). High values of T_i are associated with more transparent films with a more homogeneous refractive index through their structure, whereas lower T_i values correspond to more opaque films with heterogeneous networks. A similar pattern was observed for every film over the considered wavelength range and there were only small differences in the T_i values. The greatest differences appeared at low wavelength in aged HPMC films, indicating the development of some yellowness. Table 1 shows the T_i values at 450 nm (in the range where the greatest differences among films were observed) where, in newly prepared films, the highest T_i values were found for non-microfluidized pure HPMC and the lowest value for microfluidized pure starch films. In both films, microfluidized and non-microfluidized, the increase in the starch ratio gave rise to a decrease in transparency. In every case microfluidization provoked a decrease in the film transparency, although in pure starch films this was not significant. Nevertheless, differences are small

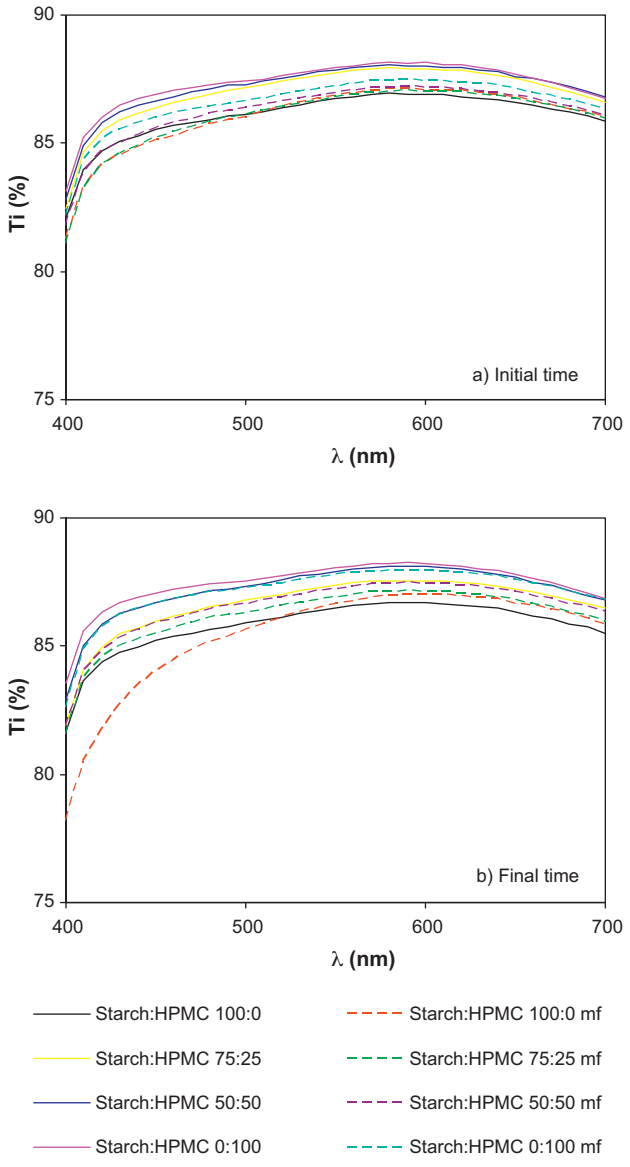

Fig. 3. Spectral distribution of internal transmittance (T_i) of microfluidized (mf) and non-microfluidized films containing different starch:HPMC ratios: (a) newly prepared and (b) conditioned films after 5 storage weeks.

and it can be concluded that HPMC addition and phase separation introduces little discontinuities in the refractive index of the polymer network, thus having only a slight impact on the film transparency. Moreover, the greater transparency of HPMC helps to lend a more transparent character to the starch films, which are more opaque. This is probably due to the fact that they are also composite films made from amylose and amylopectin fractions.

Throughout storage, small changes in film transparency occurred mainly in microfluidized pure starch and pure HPMC films. In this sense, it is remarkable that starch films became more opaque, whereas HPMC films became more transparent. Taking into account the spectral distribution (between 400 and 500 nm) of T_i corresponding to microfluidized pure starch at initial (Fig. 3B) and final time (Fig. 3B), the T_i decrease is associated with the change in this distribution and was coherent with the yellowness which could be visually observed in samples stored for 5 weeks. This could be attributed to the partial starch hydrolysis during microfluidization, which yielded brown compounds through the reaction of low

Table 1
Optical properties of both non-stored (initial) starch-HPMC based films and stored for 5 weeks (final). Samples A to D: non-microfluidized. Samples E to H: microfluidized. Mean values (standard deviation).

Sample	Starch:HPMC ratio	T_i (450 nm)		Gloss 60°	
		Initial	Final	Initial	Final
A	100:0	85.54 (0.36)^{ab1}	85.21 (0.09)^{a1}	71 (5)^{a1}	67 (9)^{a1}
B	75:25	86.38 (0.22)^{cd1}	85.97 (0.42)^{bc1}	10.32 (0.41)^{b1}	10 (1)^{b1}
C	50:50	86.66 (0.25)^{cd1}	86.69 (0.34)^{cd1}	19.15 (2.71)^{c1}	14.1 (1)^{b2}
D	0:100	86.9 (0.3)^{d1}	87.08 (0.36)^{d1}	71 (5)^{a1}	57 (9)^{c2}
E	100:0	85.12 (0.14)^{a1}	84.03 (0.33)^{e2}	65.5 (4.3)^{d1}	53.8 (8.4)^{c2}
F	75:25	85.23 (0.27)^{a1}	85.5 (0.6)^{ab1}	12.3 (0.5)^{b1}	16.1 (1.6)^{b2}
G	50:50	85.6 (0.5)^{ab1}	85.9 (0.2)^{ab1}	40.34 (4.85)^{e1}	29 (8)^{d2}
H	0:100	86.03 (0.17)^{bc1}	86.69 (0.14)^{d2}	85.24 (1.84)^{f1}	60 (9)^{ac2}

Different superscript letters within the same column indicate significant differences among formulations ($p < 0.05$).
Different superscript numbers within the same row indicate significant differences due to storage time ($p < 0.05$).

molecular weight sugars. These sugars can react to some extent in the amorphous film, at low water activity, through the complex caramelization reactions giving rise to brown compounds (Claude & Ubbink, 2006). The increase in transparency of HPMC films during storage suggests that a rearrangement of the polymer chains takes place during this time, since the film is not in a glassy state and molecular mobility permits the changes in the chain entanglements, leading to modifications in macroscopic film properties.

The obtained gloss values of newly prepared and stored films measured at an incidence angle of 60° are shown in Table 1. In all newly prepared films, the gloss values of pure HPMC or pure starch films were the highest, whereas composite films showed very low values coinciding with the roughness of the composite film surface, as observed by SEM (Fig. 2), caused by phase separation. The rougher topography is directly related with the loss of gloss (Ward & Nussinovitch, 1996). In general, microfluidization produced an increase in gloss values, except in the case of pure starch films where a decrease was observed and composite films with a 50:50 ratio of polymers, where no significant changes were induced. For composite films, these results are coherent with what can be observed in surface SEM micrographs, where a high level of roughness could be deduced for the film surface. In the case of starch, microfluidization can promote hydrolysis and recrystallization which will affect the film surface topography. In this sense, Augustin, Sanguansri, & Htoon (2008) observed that in the case of microfluidization of heated starch, there is an increase in the depolymerization of the starch chain with increasing microfluidization pressure.

As far as ageing is concerned, the films generally lost gloss probably due to a molecular rearrangement which took place during storage at 25 °C and which modifies film surface topography. Similar effects were observed by Jiménez et al. (2012) working with starch-fatty acid films.

3.3. Tensile properties

The mechanical properties of studied films were obtained at 25 °C and 53% RH. According to McHugh and Krochta (1994), elasticity modulus (EM), tensile strength (TS) and elongation at break (E) are useful parameters with which to describe the mechanical behaviour of films, and are closely related with its internal structure. The values of the tensile parameters are shown in Table 2. In newly prepared films, pure HPMC films showed the highest EM and TS values, while pure starch formulations and starch:HPMC blend films were less rigid and mechanically resistant. The presence of glycerol greatly reduced EM and TS values of HPMC films when these values are compared to those reported by Jiménez et al. (2010) for HPMC films prepared without glycerol, which must be attributed to the plasticizing effect and the subsequent increase in molecular mobility, providing more stretchable films (Arvanitoyannis, Nakayama, & Aiba, 1998; Mali et al., 2006; Rodríguez, Osés, Ziani, & Maté, 2006). This effect has also been reported in starch based films containing plasticizers (Talja et al., 2007). Microfluidization induced a decrease in EM values in almost all of the cases which could be related with the disaggregation/fragmentation of polymer chains due to the high pressure effects, as reported by Augustin et al. (2008), which affect the network compactness and rigidity. With respect to TS values, no significant effect of microfluidization was observed.

The stretchability of films at initial time ranged between 5.7 and 10.4% with no significant differences between formulations ($p > 0.05$). These values are in agreement with previous works in which films based on corn starch (Mali et al., 2006) or HPMC (Jiménez et al., 2010) were characterized. Microfluidization did not induce significant modification of the stretchability values.

Table 2 also shows mechanical parameters of stored films. The EM values were similar, or lower, in comparison with those obtained for newly prepared films, except for non-microfluidized pure starch films where a notable increase in this value was observed. This increase in the pure starch film rigidity was attributed to the recrystallization process occurring in the starch matrix, as reported by Jiménez et al. (2012) on the basis of the X-ray data. The obtained X-ray data commented below confirms this hypothesis. On the contrary, a notable decrease of EM values of microfluidized pure starch film was observed, which could indicate that no re-crystallization took place in the film throughout storage time. Microfludization promotes starch hydrolysis, thus limiting the rearrangement of amylose and amylopectin fractions in the matrix.

When HPMC was incorporated into starch films the increase in EM values, associated to starch re-crystallization, was not observed, despite the above mentioned phase separation, which suggests that HPMC addition was able to inhibit the starch re-crystallization during storage. In fact, HPMC addition was chosen as a possible mechanism to reduce the recrystallization of starch over time, thus reducing the brittleness of films after storage. As mentioned above, HPMC is characterized by its amorphous structure (Kou et al., 2011) and crystallization of the polymer during aging was not expected. Although phase separation was observed, HPMC would be present in both phases (at different concentrations) in a required amount to inhibit the crystal formation in the starch matrix.

For pure starch non microfluidized films the TS value increased, in agreement with the increase in the crystallinity developed over time, as shown in X-ray diffraction patterns (Fig. 4), commented below. A small increase was also observed for microfluidized pure HPMC films which suggest a polymer rearrangement during storage, as was also deduced from the analysis of the film transparency. In the rest of the cases no changes or only a slight decrease (in

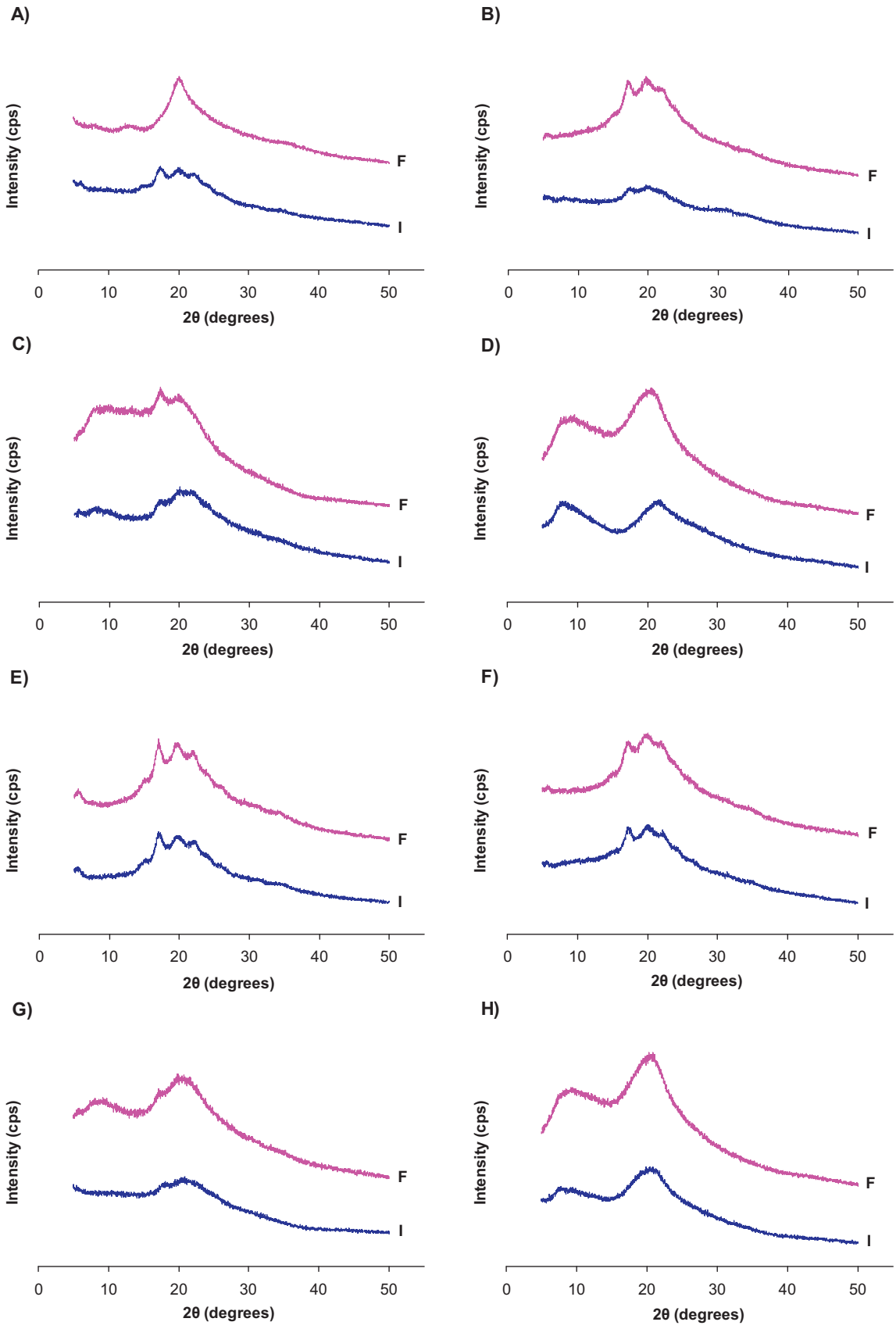

Fig. 4. X-ray diffraction patterns of newly prepared (I curve) and stored films (F curve). A to D correspond to non-microfluidized films, E to H correspond to microfluidized films. A and E: 100:0 starch:HPMC ratio, B and F: 75:25 starch:HPMC ratio, C and G: 50:50 starch:HPMC ratio and D and H: 0:100 starch:HPMC ratio.

Table 2
Tensile properties of both non-stored (initial) starch-HPMC based films and stored for 5 weeks (final). Samples A to D: non-microfluidized. Samples E to H: microfluidized. Mean values (standard deviation).

Sample	Starch:HPMC ratio	EM (MPa)		TS (MPa)		ε (%)	
		Initial	Final	Initial	Final	Initial	Final
A	100:0	806 (74)^{a1}	1474 (156)^{a2}	9.12 (0.63)^{a1}	20 (2)^{a2}	7.6 (4.4)^{abc1}	2.2 (0.2)^{a2}
B	75:25	743 (44)^{ab1}	620 (88)^{b2}	10.90 (0.33)^{ab1}	10.38 (0.35)^{b2}	7 (2)^{ab1}	11.1 (3.3)^{bc2}
C	50:50	670 (62)^{c1}	700 (28)^{c1}	13 (1)^{bc1}	13.5 (1.1)^{d1}	9.4 (1.6)^{bc1}	12.5 (1.9)^{dc2}
D	0:100	1312 (61)^{d1}	1043 (40)^{d2}	24.5 (4.5)^{d1}	23.26 (4.31)^{d1}	10.4 (4.)^{c1}	18.52 (2.27)^{e2}
E	100:0	747 (33)^{ab1}	400 (56)^{e2}	9.53 (0.43)^{a1}	6.6 (0.4)^{e2}	6.5 (2.4)^{ab1}	13.7 (2.3)^{d2}
F	75:25	593 (68)^{e1}	420 (25)^{e2}	8.58 (0.64)^{a1}	6.13 (0.34)^{e2}	5.7 (1.4)^{a1}	8.6 (2.6)^{bf2}
G	50:50	683 (49)^{bc1}	761 (59)^{c2}	12.81 (0.25)^{b1}	11.5 (1.2)^{bc1}	9.3 (2.8)^{bc1}	8.08 (1.44)^{f1}
H	0:100	1061 (51)^{f1}	1108 (32)^{d1}	15.8 (4.5)^{c1}	22.3 (4.3)^{ad2}	8.43 (4.13)^{abc1}	18.71 (3.15)^{e2}

Different superscript letters within the same column indicate significant differences among formulations ($p < 0.05$).
Different superscript numbers within the same row indicate significant differences due to storage time ($p < 0.05$).

microfluidized starch-rich films) was observed for TS values during storage.

Generally stretchability of pure starch non microfluidized films greatly decreased during storage in line with the formation of crystalline zones which limits displacements of macromolecules. Nevertheless, in the rest of the cases, stored films were more stretchable than newly prepared films, which indicate that HPMC addition or microfluidization inhibits re-crystallization phenomena, leading to less resistant but more flexible films throughout storage. So, mechanical properties of starch based films may be improved with the addition of a determined amount of HPMC or by microfluidization. To corroborate this result, crystallization of polymers in the films was characterized by means of X-ray diffraction.

Fig. 4 shows the X-ray diffraction patterns for both newly prepared and stored films. In starch containing films main peaks located around 20° appeared. These are attributed to the starch crystalline domain and this was previously observed in tapioca starch-potassium sorbate films (Famá, Rojas, Goyanes, & Gerschenson, 2005), tapioca starch-decolourized-tsao leaf gum films (Chen, Kuo, & Lai, 2009) and corn starch-fatty acids films (Jiménez et al., 2012). The intensity of the peaks increased with storage time in non-microfluidized pure starch and 50:50 polymer ratio films, but did not change in the rest of the cases, thus indicating that re-crystallization during storage was inhibited. Nevertheless crystallization during film formation also occurred in microfluidized pure starch and 50:50 polymer ratio films. Pure HPMC films showed a totally amorphous pattern in agreement with previous observations obtained by the same technique (Kou et al., 2011). These results confirm that an increase of HPMC in starch matrix or microfluidization of the film forming solutions provoke an inhibition of starch re-crystallization during storage. A 50:50 polymer ratio also allows us to inhibit starch crystallization during film formation in both microfluidized and non-microfluidized films. This behaviour coincides with that commented on above, deduced from the mechanical behaviour of the films.

3.4. Barrier properties

The ability of films or packaging to limit the transfer of environmental agents (water vapour, oxygen, CO_2) has been studied (Arvanitoyannis & Biliaderis, 1998; García, Martino, & Zaritzky, 2000; Karbowiak, Debeaufort, & Voilley, 2007; Mali et al., 2006; Navarro-Tarazaga, Massa, & Pérez-Gago, 2011; Souza et al., 2009) and reviewed by many researchers (Koelsch, 1994; Miller & Krochta, 1997). Packaging has to be able to avoid moisture and gas exchange between the environment and the product. Both water vapour and oxygen barrier were characterized in the films, both newly prepared and conditioned and after five storage weeks. WVP and OP values are shown in Table 3. WVP values ranged between 5.21 and 10.3 g mm kPa^{-1} h^{-1} m^{-2} considering both initial and final time. These results agree with those from previous studies in which starch films were obtained. For instance, Pushpadass, Marx, & Hanna (2008) obtained WVP values between 10.9 and 12.9 g mm kPa^{-1} h^{-1} m^{-2} in starch films containing stearic acid and Jiménez et al. (2012) between 6.71 and 9.14 g mm kPa^{-1} h^{-1} m^{-2} in starch-fatty acid films.

The obtained values for newly prepared non-microfluidized films did not show a clear tendency with the HPMC content since both pure starch and HPMC showed very similar values, in agreement with their very similar hydrophilic character. Microfluidization slightly decreases WVP, which is coherent with the structural effects commented on above (chain disaggregation/fragmentation and formation of a less compact network).

Concerning to the effect of storage time, WVP values generally did not change, or only slightly increased which can be due to the polymer rearrangements commented on above, associated to matrix ageing. For pure starch microfluidized films WVP decreased significantly ($p < 0.05$) over storage time, as reported by Mali et al. (2006) for corn, cassava and yam starch. This decrease in WVP values of starch stored films could be explained by a progressive hydrolysis of the starch which led to the formation of a less compact network where small molecule permeation can occur more easily. Hydrolysis of starch is promoted by the effect of shear stress forces (Carvalho, 2008; Myllymäki et al., 1997), such as those applied in microfluidization. Likewise, some authors (Courgneau, Domenek, Guinault, Avérous, & Ducruet, 2011) reported that polyols (such as glycerol) as long as they plasticize the biopolymer matrix, they favour crystallization because of polymer mobility increase and, in some biopolymer matrices such as PLA, also induce chain length reduction (measured by size exclusion chromatography) in parallel to crystallization. The reduction of the polymer chain length will induce a lower permeability.

In order to evaluate the ability of films to limit oxygen transfer, the oxygen permeability (OP) was analysed at 53% HR and 25 °C. Obtained values for OP are shown in Table 3 as mentioned above. Starch films have better oxygen barrier properties than HPMC films, so oxygen permeability greatly increased when HPMC ratio increased in the films. In newly prepared films, microfluidization gave rise to an increase in oxygen permeability of pure HPMC films and a decrease in the 50:50 polymer ratio films, but no changes in other cases. The obtained values for films containing were lower in comparison with those reported for sodium caseinate-starch films (Arvanitoyannis & Biliaderis, 1998) and for corn starch:cellulose:lignin composites (Wu, Wang, Li, Li, & Wang, 2009).

The effect of storage time on oxygen permeability depended on the film composition and the homogenization process. In most

Table 3
Water vapour and oxygen permeability of both non-stored (initial) starch-HPMC based films and stored films for 5 weeks (final). Samples A to D: non-microfluidized. Samples E to H: microfluidized. Mean values (standard deviation).

Sample	Starch:HPMC ratio	WVP (g mm kPa^{-1} h^{-1} m^{-2})		O_2 perm. 10^{14} (cm^3 m^{-1} s^{-1} Pa^{-1})	
		Initial	Final	Initial	Final
A	100:0	7.9 (0.2)^{a1}	7.7 (0.9)^{ab1}	4 (4)^{ab1}	4.2 (0.4)^{a1}
B	75:25	7.13 (0.36)^{b1}	8.6 (0.3)^{a2}	10.67 (0.06)^{b1}	17.7 (0.3)^{a2}
C	50:50	8.5 (0.4)^{a1}	7.6 (0.4)^{ab1}	27.5 (0.5)^{c1}	31.1 (2.5)^{a1}
D	0:100	8.32 (0.43)^{a1}	8.5 (0.5)^{a1}	285 (4)^{d1}	740 (88)^{b2}
E	100:0	6.24 (0.43)^{c1}	5.2 (0.3)^{c2}	2.22 (0.05)^{a1}	4.15 (0.18)^{a2}
F	75:25	7.16 (0.64)^{b1}	10.3 (1.0)^{d2}	7.9 (1.5)^{ab1}	17.4 (0.8)^{a2}
G	50:50	5.95 (0.28)^{c1}	7.9 (0.8)^{ab2}	8 (1)^{ab1}	21 (2)^{a2}
H	0:100	6.95 (0.23)^{b1}	7.3 (0.6)^{b1}	566 (7)^{e1}	573 (40)^{c1}

Different superscript letters within the same column indicate significant differences among formulations ($p < 0.05$).
Different superscript numbers within the same row indicate significant differences due to storage time ($p < 0.05$).

of the cases an increase in the OP values was observed, mainly in microfluidized composite films and in non-microfluidized pure HPMC films. This must be explained by the microstructural rearrangement of the polymer chains during storage.

4. Conclusions

The addition of HPMC into the corn starch matrix gave rise to a more amorphous structure as was observed by X-ray diffraction. However, SEM micrographs revealed a polymer phase separation which provoked a loss of gloss in the films. Elastic modulus of newly prepared composite films decreased as compared to pure starch and HPMC films although tensile strength and deformation at break are slightly improved with respect to pure starch film. Composite films showed similar WVP to pure starch films but slightly higher oxygen permeability due to the contribution of the HPMC which showed high OP values. Microfluidization did not allow the homogenous mixture of both polymers, which showed phase separation in the films, but contributed to the inhibition of starch re-crystallization during storage, giving rise to slightly less rigid films with similar resistance to break and stretchability. Inhibition of the starch re-crystallization during film formation and storage was also reached in both microfluidized and non-microfluidized films when HPMC was incorporated to starch films in a 50:50 ratio.

Acknowledgements

The authors acknowledge the financial support from the Spanish Ministerio de Economía y Competitividad throughout the project AGL2010-20694, co-financed with FEDER funds. A. Jiménez also thanks Conselleria de Educació de la Comunitat Valenciana for the FPI grant. Author M.J. Fabra thanks the support of Campus de Excelencia Internacional from Universitat Politècnica de València.

References

Annable, P., Fitton, M. G., Harris, B., Philips, G. O., & Williams, P. A. (1994). Phase behaviour and rheology of mixed polymer systems containing starch. *Food Hydrocolloids*, *8*(4), 351–359.

Arvanitoyannis, I., & Biliaderis, C. G. (1998). Physical properties of polyol-plasticized edible films made from sodium caseinate and soluble starch blends. *Food Chemistry*, *62*(3), 333–342.

Arvanitoyannis, I., Nakayama, A., & Aiba, S. (1998). Edible films made from hydroxypropyl starch and gelatine and plasticized by polyols and water. *Carbohydrate Polymers*, *36*(2–3), 105–119.

ASTM. (1995). Standard test methods for water vapour transmission of materials. In *Annual book of ASTM standards*. Philadelphia, PA: American Society for Testing and Materials., pp. 406–413 (Standard Designations: E96-95).

ASTM. (1999). *Standard test method for specular gloss. Annual book of ASTM standards* Philadelphia, PA: American Society for Testing and Materials. Designation (D523).

ASTM. (2001). Standard test method for tensile properties of thin plastic sheeting. In *Annual book of American Standard Testing Methods*. Philadelphia, PA: American Society for Testing and Materials., pp. 162–170 (Standard D882).

ASTM. (2002). Standard test method for oxygen gas transmission rate through plastic film and sheeting using a coulometric sensor (D 3985-95). In *Annual book of ASTM standards*. Philadelphia, PA: American Society for Testing and Materials., pp. 472–477.

Augustin, M. A., Sanguansri, P., & Htoon, A. (2008). Functional performance of a resistant starch ingredient modified using a microfluidiser. *Innovative Food Science & Emerging Technologies*, *9*(2), 224–231.

Bertuzzi, M. A., Armada, M., & Gottifredi, J. C. (2007). Physicochemical characterization of starch based films. *Journal of Food Engineering*, *82*(1), 17–25.

Bilbao-Sainz, C., Bras, J., Williams, T., Sénechal, T., & Orts, W. (2011). HPMC reinforced with different cellulose nano-particles. *Carbohydrate Polymers*, *86*(4), 1549–1557.

Bourtoom, T., & Chinnan, M. S. (2008). Preparation and properties of rice starch-chitosan blend biodegradable film. *LWT – Food Science and Technology*, *41*(9), 1633–1641.

Carvalho, A. J. F. (2008). Starch: Major sources, properties and applications as thermoplastic materials. In M. N. Belgacem, & A. Gandini (Eds.), *Monomers, polymers and composites from renewable resources* (pp. 321–342). Amsterdam, Holland: Elsevier.

Chen, C., Kuo, W., & Lai, L. (2009). Rheological and physical characterization of film-forming solutions and edible films from tapioca starch/decolorized hsian-tsao leaf gum. *Food Hydrocolloids*, *23*(8), 2132–2140.

Chillo, S., Flores, S., Mastromatteo, M., Conte, A., Gerschenson, L., & Del Nobile, M. A. (2008). Influence of glycerol and chitosan on tapioca starch-based edible film properties. *Journal of Food Engineering*, *88*(2), 159–168.

Claude, J., & Ubbink, J. (2006). Thermal degradation of carbohydrate polymers in amorphous states: A physical study including colorimetry. *Food Chemistry*, *96*(3), 402–410.

Courgneau, C., Domenek, S., Guinault, A., Avérous, L., & Ducruet, V. (2011). Analysis of the structure-properties relationships of different multiphase systems based on plasticized poly(lactic acid). *Journal of Polymers and the Environment*, *19*(2), 362–371.

Fabra, M. J., Talens, P., & Chiralt, A. (2009). Microstructure and optical properties of sodium caseinate fims containing oleic acid-beeswax mixtures. *Food Hydrocolloids*, *23*(3), 676–683.

Fabra, M. J., Jiménez, A., Atarés, L., Talens, P., & Chiralt, A. (2009). Effect of fatty acids and beeswax addition on properties of sodium caseinate dispersions and films. *Biomacromolecules*, *10*, 1500–1507.

Fahs, A., Brogly, M., Bistac, S., & Schmitt, M. (2010). Hydroxypropyl methylcellulose (HPMC) formulated films: Relevance to adhesion and friction surface properties. *Carbohydrate Polymers*, *80*(1), 105–114.

Falguera, V., Quintero, J. P., Jiménez, A., Muñoz, J. A., & Ibarz, A. (2011). Edible films and coatings: Structures, active functions and trends in their use. *Trends in Food Science & Technology*, *22*(6), 292–303.

Famá, L., Rojas, A. M., Goyanes, S., & Gerschenson, L. (2005). Mechanical properties of tapioca-starch edible films containing sorbates. *LWT – Food Science and Technology*, *38*(6), 631–639.

Flores, S., Conte, A., Campos, C., Gerschenson, L., & Del Nobile, M. (2007). Mass transport properties of tapioca-based active edible films. *Journal of Food Engineering*, *81*(3), 580–586.

García, M. A., Martino, M. N., & Zaritzky, N. E. (2000). Lipid addition to improve barrier properties of edible starch-based films and coatings. *Journal of Food Science*, *65*(6), 941–947.

García, M. A., Pinotti, A., Martino, M. N., & Zaritzky, N. E. (2009). Characterization of starch and composite edible films and coatings. In *Edible films and coatings for food applications*. Springer., pp. 169–209.

Huang, H. C., Chen, L. C., Lin, S. B., & Chen, H. H. (2011). Nano-biomaterials application: In situ modification of bacterial cellulose structure by adding HPMC during fermentation. *Carbohydrate Polymers*, *83*(2), 979–987.

Hutchings, J. B. (1999). *Food and colour appearance* (2nd ed.). Gaithersburg, MD: Chapman and Hall Food Science Book, Aspen Publication.

Jiménez, A., Fabra, M. J., Talens, P., & Chiralt, A. (2010). Effect of lipid self-association on the microstructure and physical properties of hydroxypropyl-methylcellulose edible films containing fatty acids. *Carbohydrate Polymers*, *82*(3), 585–593.

Jiménez, A., Fabra, M. J., Talens, P., & Chiralt, A. (2012). Effect of re-crystallization on tensile, optical and water vapour barrier properties of corn starch films containing fatty acids. *Food Hydrocolloids*, *26*(1), 302–310.

Karbowiak, T., Debeaufort, F., & Voilley, A. (2007). Influence of thermal process on structure and functional properties of emulsion-based edible films. *Food Hydrocolloids*, *21*(5–6), 879–888.

Koelsch, C. (1994). Edible water vapor barriers: Properties and promise. *Trends in Food Science and Technology*, *5*(3), 76–81.

Kou, W., Cai, C., Xu, S., Wang, H., Liu, J., Yang, D., et al. (2011). In vitro and in vivo evaluation of novel immediate release carbamazepine tablets: Complexation with hydroxypropyl-β-cyclodextrin in the presence of HPMC. *International Journal of Pharmaceutics*, *409*(1–2), 75–80.

Kuorwel, K. K., Cran, M. J., Sonneveld, K., Miltz, J., & Bigger, S. W. (2011). Antimicrobial activity of biodegradable polysaccharide and protein-based films containing active agents. *Journal of Food Science*, *76*(3), 90–102.

Liu, P., Yu, L., Wang, X., Li, D., Chen, L., & Li, X. (2010). Glass transition temperature of starches with different amylose/amylopectin ratios. *Journal of Cereal Science*, *51*(3), 388–391.

Mali, S., Grossmann, M. V. E., García, M. A., Martino, M. N., & Zaritzky, N. E. (2006). Effects of controlled storage on thermal, mechanical and barrier properties of plasticized films from different starch sources. *Journal of Food Engineering*, *75*(4), 453–460.

Mathew, S., & Abraham, T. E. (2008). Characterisation of ferulic acid incorporated starch-chitosan blend films. *Food Hydrocolloids*, *22*(5), 826–835.

McHugh, T. H., Avena-Bustillos, R., & Krochta, J. M. (1993). Hydrophilic edible films: modified procedure for water vapour permeability and explanation of thickness effects. *Journal of Food Science*, *58*(4), 899–903.

McHugh, T. H., & Krochta, J. M. (1994). Water vapor permeability properties of edible whey protein–lipid emulsion films. *Journal of the American Oil Chemists' Society*, *71*(3), 307–312.

Miller, K. S., & Krochta, J. M. (1997). Oxygen and aroma barrier properties of edible films: A review. *Trends in Food Science and Technology*, *8*(7), 228–237.

Navarro-Tarazaga, M. L., Massa, A., & Pérez-Gago, M. B. (2011). Effect of beeswax content on hydroxypropyl methylcellulose-based edible film properties and postharvest quality of coated plums (Cv. Angeleno). *LWT – Food Science and Technology*, *44*(10), 2328–2334.

Myllymäki, O., Eerikäinen, T., Suortti, T., Forssell, P., Linko, P., & Poutanen, K. (1997). Depolymerization of barley starch during extrusion in water glycerol mixtures. *LWT – Food Science and Technology*, *30*(4), 351–358.

Paes, S. S., Yakimets, I., & Mitchell. (2008). Influence of gelatinization process on functional properties of cassava starch films. *Food Hydrocolloids*, *22*(5), 788–797.

Phan The, D., Debeaufort, F., Luu, D., & Voilley, A. (2005). Functional properties of edible agar-based and starch-based films for food quality preservation. *Journal of Agricultural and Food Chemistry*, *53*(4), 973–981.

Phan The, D., Debeaufort, F., Voilley, A., & Luu, D. (2009). Biopolymer interactions affect the functional properties of edible films based on agar, cassava starch and arabinoxylan blends. *Journal of Food Engineering*, *90*(4), 548–558.

Pushpadass, H. A., Marx, D. B., & Hanna, M. A. (2008). Effects of extrusion temperature and plasticizers on the physical and functional properties of starch films. *Starch/Stärke*, *60*, 527–538.

Rindlav-Westling, Å., Stading, M., & Gatenholm, P. (2002). Crystallinity and morphology in films of starch, amylose and amylopectin blends. *Biomacromolecules*, *3*(1), 84–91.

Rodríguez, M., Osés, J., Ziani, K., & Maté, J. I. (2006). Combined effect of plasticizers and surfactants on the physical properties of starch based edible films. *Food Research International*, *39*(8), 840–846.

Souza, B. W. S., Cerqueira, M. A., Casariego, A., Lima, A. M. P., Teixeira, J. A., & Vicente, A. A. (2009). Effect of moderate electric fields in the permeation properties of chitosan coatings. *Food Hydrocolloids*, *23*(8), 2110–2115.

Talja, R. A., Helén, H., Roos, Y. H., & Jouppila, K. (2007). Effect of various polyols and polyol contents on physical and mechanical properties of potato starch-based films. *Carbohydrate Polymers*, *67*(3), 288–295.

Tang, X., Alavi, S., & Herald, T. J. (2008). Barrier and mechanical properties of starch-clay nanocomposite films. *Cereal Chemistry*, *85*(3), 433–439.

Vásconez, M. B., Flores, S. K., Campos, C. A., Alvarado, J., & Gerschenson, L. N. (2009). Antimicrobial activity and physical properties of chitosan-tapioca starch based edible films and coatings. *Food Research International*, *42*(7), 762–769.

Villalobos, R., Chanona, J., Hernández, P., Gutiérrez, G., & Chiralt, A. (2005). Gloss and transparency of hydroxypropyl methylcellulose films containing surfactants as affected by their microstructure. *Food Hydrocolloids*, *19*(1), 53–61.

Ward, G., & Nussinovitch, A. (1996). Gloss properties and surface morphology relationships of fruits. *Journal of Food Science*, *61*(5), 973–977.

Wu, R. L., Wang, X. L., Li, F., Li, H. Z., & Wang, Y. Z. (2009). Green composite films prepared from cellulose, starch and lignin in room-temperature ionic liquid. *Bioresource Technology*, *100*, 2569–2574.

Zhu, L. J., Liu, Q. Q., Wilson, J. D., Gu, M. H., & Shi, Y. C. (2011). Digestibility and physicochemical properties of rice (*Oryza sativa* L.) flours and starches differing in amylose content. *Carbohydrate Polymers*, *86*(4), 1751–1759.